Journal of Mines, Metals and Fuels, *71(12D) : 274-279; 2023. DOI: 10.18311/jmmf/2023/48343*

Print ISSN : 0022-2755

Journal of Mines, Metals and Fuels

Contents available at: *www.informaticsjournals.com/index.php/jmmf*

Study of Process Parameters of Abrasive Water Jet Cutting Machine on ZA 27 using Design of Experiments

B. S. Aishwarya*, N. D. Prasanna, S. Hamritha*, C. A. Niranjan and Ayushi Chatterji

Department of Industrial Engineering and Management, M S Ramaiah Institute of Technology, Bengaluru – 560054, Karnataka, India; bsaishwarya30@gmail.com, nd.prassana47@gmail.com, hamritha.ap@gmail.com, niranjancaster@gmail.com, ayushichatterjee9@gmail.com

Abstract

In the current work, abrasive water jet cutting parameters on surface roughness were identified through experimental inquiry on the aluminium alloy ZA 27. L9 Orthogonal array was used to evaluate the impact of input parameters such as water pressure, traverse speed, and mass flow rate on the surface integrity of the ZA 27 aluminium alloy. To determine the cutting mechanism responsible for producing smooth and rough surfaces, SEM investigations were conducted on the cut surfaces. The surface roughness was measured using a non-contact 3D optical profiler of the Taylor Hobson type. From the results, it can be inferred that water jet pressure and traverse speed have a greater impact on surface quality, i.e., an increase in water pressure results in an improvement in surface quality, while a decrease in traverse speed leads in an improvement. Although mass flow rate alone has the least impact on surface quality, when combined with other significant influencing factors like traverse speed and water jet pressure, mass flow rate improves surface quality. From SEM, it was discovered that micro-cutting was influenced by cutting particles with a sharp edge on the smooth cutting zone. While waviness and deviating wear tracks brought about by a diverted water jet affected the rough cutting zone. Shallow impact angles revealed the embedment of spherical garnet particles on the rough cutting zone. With a water pressure of 200 psi, a traverse speed of 40 minutes, and a mass flow rate of 300 g/mm, the highest surface of 3.038 m was reached. It is clear that the surface quality of the ZA 27 alloy will improve with rising water pressure and slow traverse rates.

Keywords: *Abrasive Water Jet Cutting, L9 Orthogonal Array, Process Parameters, ZA 27*

1.0 Introduction

The efficiency of any vehicle might be greatly improved by using lightweight materials. Two potential lightweight materials that are frequently employed in engineering applications are aluminium and magnesium. Al is the 2nd highest structural material next to magnesium, which has a density of 2.7 g/cm^3, compared to cast iron's 7.2 g/cm^3 and zinc's 7.3 g/cm^3 [1]. It's a very versatile metal that can be cast melted, moulded, machined, and extruded. Due to high specific strength and low density, it has excellent castability, thermal conductivity, resistance to corrosion, and can be machined and moulded quickly. In the recent years Aluminium alloys has gained wide acceptance among the industries as its mechanical and tribological properties are enhanced with the use of different types of reinforcements. For high load, low speed power transmission applications, Zinc Aluminium (ZA) alloys are predominantly used in journal bearings. These alloys may, and frequently do, replace conventional bronze bearings.

*Author for correspondence

ZA is a silvery coloured alloy and has unparalleled bearing properties. Common ZA alloy includes ZA8, ZA12, and ZA27, where the numeric indicates the amount of aluminium and zinc contained it[2]. Among the three ZA alloys, ZA-27 alloys are widely used. ZA 27 is the considered to be the best bearing material for low pressure and high speeds. The affordability of ZA-27 alloy is another key benefit[3]. Additionally, ZA-27 is less susceptible to load variations and heavy impact loads. Since ZA is a natural lubricant for smaller components, it could be possible to do away with wear inserts and small bushings, which would reduce the cost of secondary manufacturing[4]. Due to the low casting temperatures, the residual stresses in ZA alloy are often at their lowest. Materials from ZA can be polished to a shiny, chrome-like sheen that can be lacquered for durability[5].

The performance of any material on machinability and industrial applications of such materials are based on eased of machinability. The type of material used for the work piece, thickness, machining capabilities, and cut surface quality should all be taken into consideration while choosing the cutting technology[6]. In traditional machining, material from the work piece is removed via shear deformation during the machining process to create the desired shape. However, majority of the materials undergo conventional machining process and are affected by heat affected zone, that creates numerous problems like reduction in quality of machined surface, formation of built-up edges, altering microstructure and some even alter the performance where high operating temperatures are involved. Unconventional metal cutting machining are Electrochemical Machining (ECM), Laser Machining (LAM), and abrasive water jet water machining, have been developed to address this issue with conventional machining techniques (AWJM). The advantage of AWJM are absence of thermal distortion, absence of potential for fire hazards, greater flexibility, and it doesn't alter material properties[7]. In industrial applications the depth of penetration and surface quality are crucial to determine the effectiveness, performance, and process capabilities of water jet machining process. The AWJ technique has been used to cut the earth's hard materials, including diamond, granite, marbles, and various stones. Using water jet cutting, sculptures and decorative things are created. In this work, ZA 27 was cut utilizing AWJM procedure by adjusting the traverse speed of the nozzle, pressure of water, standoff distance and mass flow rate of the abrasives. To attain the lowest surface roughness possible while cutting the ZA 27 alloy, Taguchi method is examined. Initial damage, smooth and rough-cut zones are the three areas on the cut surface where surface roughness is examined.

2.0 Materials and Methods

ZA alloy was prepared using die casting in the dimensions of 60mm*50mm*40mm. The chemical composition of ZA is given in Table 1. SEM images were used to analyze the cut surface and Taylor and Hobson 3D surface optical profiler was used to measure the roughness in terms of Ra µm.

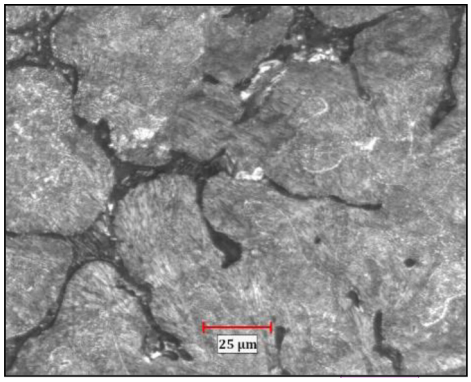


Figure 1. Microstructure and elements present in the alloy.

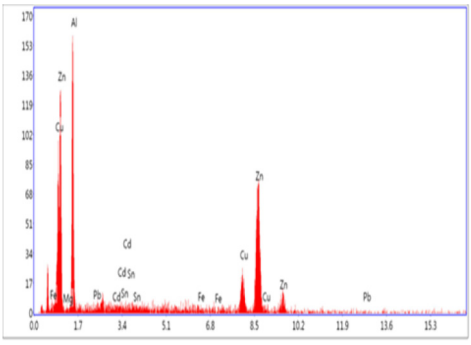


Figure 2. Elements present in the alloy.

Table 1. Chemical Composition of ZA 27

Element	ZnL	MgK	AlK	CdL	SnL	FeK	CuK	PbL
Weight %	46.03	0.45	33.23	0.75	0.55	1.48	12.00	5.50

In AWJM process abrasive water jet nozzle, water pumping system, abrasive feed system, and catcher are often used[8]. The pressure of water is increased by the pumping system to supply high velocity water. In the nozzle, momentum is transferred from the water jet to the abrasive and the mixing process takes place.

The key input factors that simulates the surface roughness of the material employed in the study are traversal speed, water pressure, and standoff distance. Abrasives used in this experiment is garnet. Average surface roughness is considered in this studied in terms of Ra. ZA 27 is alloy, which is used to study the process parameters of AWJC[9]. The specimen is initially cut in the AWJC machine and the specimens required are cut with the help of wire cut machine as shown in Figures 3 and 4.

Three process parameters of AWJM namely, water pressure, traverse speed and mass flow rate are considered to study the surface roughness of ZA 27. The study is conducted using parameters as shown in Table 2.

The categories on the cut surfaces are initial damage zone, smooth and rough-cut zones. Smooth cutting zone and rough cutting zone, are used to categorise cut surfaces in AWJM. The surfaces of IDZ are free of imperfections and wear traces. Due to frequent impacts from water jet and sharp-edged abrasive particles, the surface roughness at this zone is typically lower. The SCZ's surfaces are initially clear and flat, but the bottom half of the SCZ is damaged by direction of jet traverse and produces uniform wear tracks. Surface roughness rises deeper down the surfaces because this zone is shared by both micro cutting and distortion modes. Only SCZ and RCZ parameters are taken into account in the current zone, leaving IDZ out[10-12].

Impact of input parameters is analyzed using L9 orthogonal array. In order to optimize the process parameters of an experiment, orthogonal array is one of the simplest and effective tools[13-15]. The OA offers the most tests and calculations for the S/N Ratio (SNR). Taguchi method converts the objective function to SNR, which is the prime measure of the performance features of the

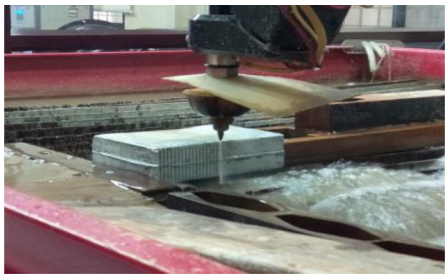


Figure 3. Abrasive water jet cutting machine.



Figure 4. Wire cut machining process.

Table 2. Process parameters of AWJM

Levels	Water Pressure (WP) (Psi)	Traverses Speed (TS) (min)	Mass Flow Rate (MFR) (g/min)
1	200	30	200
2	250	40	300
3	300	50	400

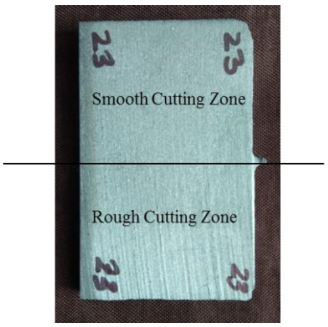


Figure 5. Cut Sample of ZA27 using AWJM.

Table 3. Orthogonal array L9

Levels	Water Pressure	Traverses Speed	Mass Flow Rate
1	200	30	200
2	200	40	300
3	200	50	400
4	250	30	300
5	250	40	400
6	250	50	200
7	300	30	400
8	300	40	200
9	300	50	300

experimentation work. Table 3, shows the L9 orthogonal array used in this work to analyze the impact on surface roughness.

The specimens obtained from the said experiments surface roughness are studied using optical profiler. It is a metrology instrument used to characterize the upper layer of the components. The output obtained is the sub-micron (µm) textural variations of its surface and characterized as surface roughness. The setup is as shown in Figures 6 and 7.

3.0 Results and Discussions

When employing an abrasive water jet cutting machine, the effect of process variables including pressure of water, speed of nozzle, and mass flow rate of the abrasive on the surface of ZA 27 alloy is investigated. The surface roughness primary effect charts are displayed in Figures 8 and 9.

Further the samples are cut in the AWJM in the desired size to analyse the roughness on the surface of the samples. The cut sample is as shown in the Figure 4. The roughness on the surface of the samples is studied using L9 orthogonal array. The cut samples have two zones namely rough-cut zones and smooth cut zones. Wear tracks are strayed along with curliness brought on by diverted water jet is observed in the rough-cut zone. At the shallow impact angles, pockets and other similar structures are seen embedded with spherical abrasive particles. In comparison to other zones, this zone has rougher surfaces. The profile images of the above test are shown in Figure 10. In RCZ, surfaces appear to be irregular and affected by striation marks (indicated in red colour). The distribution of peaks in RCZ is found non-uniform due to the variations in the depth of peaks. Surface roughness in RCZ found to be higher due to the higher traverse speeds. Similarly, SCZ the surfaces are free from striations and distribution of peaks in SCZ was found to be uniform (indicated in blue colour). Nine samples surface roughness is tested using non-contact test equipment – Taylor Hobson and the surface roughness values obtained Ra are tabulated as shown in Figure 10.

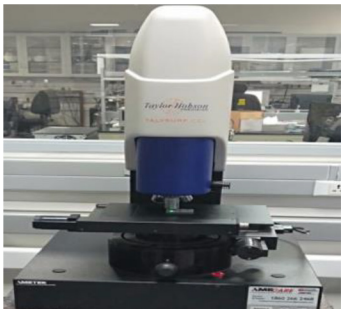


Figure 6. Taylor Hobson equipment - optical profiler.

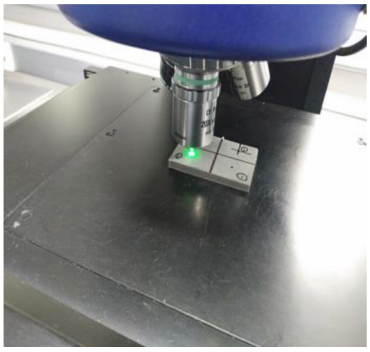


Figure 7. Optical profiler testing surface.

3.1 Water Pressure's Impact on Surface Roughness

With increased water pressure, it was found that the machined surface's roughness was decreased. The surface finish is significantly influenced by jet pressure. Surface smoothness rises with jet pressure. With increase in the jet pressure the brittle abrasives disintegrate into smaller

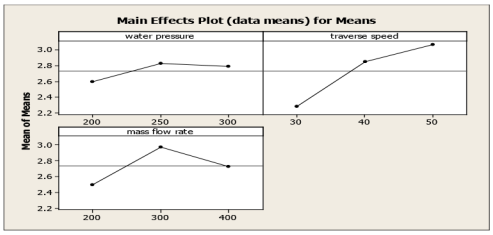


Figure 8. Main effect plots of Ra for SCZ.

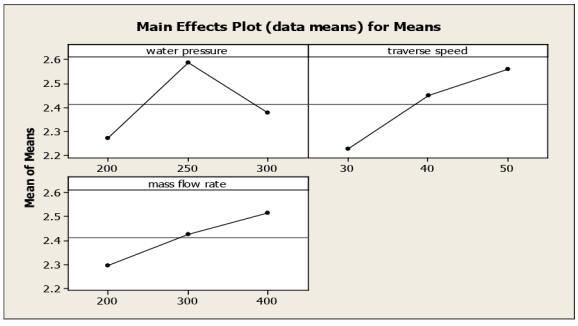


Figure 9. Main effect plots of Ra for RCZ.

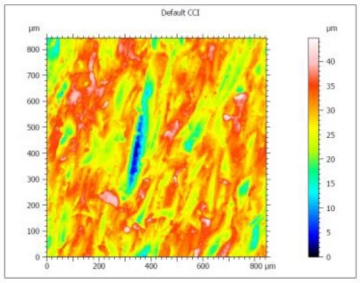
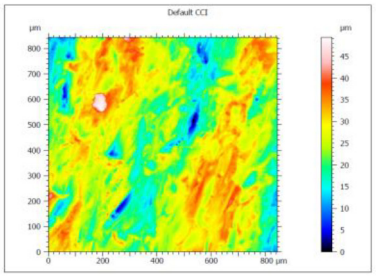
Zones	2D images
RCZ	
SCZ	

Figure 10. SEM image of cut surface

Table 4. Ra Mean values of smooth and rough cut zones

Levels	Pressure (Psi)	Traverses speed (min)	Mass flow rate (g/min)	Smooth Cut Zone(µm)	Rough Cut Zone (µm)
1	200	30	200	1.854	1.778
2	200	40	300	3.038	2.529
3	200	50	400	2.879	2.504
4	250	30	300	2.577	2.399
5	250	40	400	2.876	2.539
6	250	50	200	3.013	2.827
7	300	30	400	2.423	2.500
8	300	40	200	2.632	2.286
9	300	50	300	2.613	2.414

Table 5. Response table for Means for SCZ

Level	Pressure	Traverse speed	Mass flow rate
1	2.590	2.285	2.500
2	2.822	2.849	2.972
3	2.785	3.064	2.726
Delta	0.232	0.78	0.472
Rank	3	1	2

ones. The surface gets smoother as a result of the abrasives' size decrease. Once more, as a result of an increase in jet pressure, the particles' kinetic energy rises, producing a smoother machined surface.

Table 6. Response table for Means for RCZ

Level	Pressure	Traverse speed	Mass flow rate
1	2.270	2.226	2.297
2	2.588	2.451	2.427
3	2.380	2.561	2.514
Delta	0.318	0.336	0.217
Rank	2	1	3

3.2 Effect of Traverse Speed on Surface Roughness

The surface roughness increases with increase in traverse speed. This is because the traverse speed allows fewer abrasives to strike on the surface to yield narrower slot. Decreasing the traverse speed increases surface quality since abrasive water particles will have sufficient time to hit the target material. Repeated impact of abrasive particle at slower rate increase the surface quality on the sample. Therefore, Ra values found optimum in the zone.

3.3 Mass Flow Rate's Impact on Surface Roughness

To break down any material's bonding strength, a lot of impact must be made in per unit surface area while applying a specific amount of pressure. Surface roughness reduces as abrasive flow rate rises. This is due to the increased abrasive flow rate hitting the cutting edges per unit area. With the help of the rate of abrasive material available on the samples total available kinetic energy is determined.

As a result, the cutting power of the jet should increase with increasing abrasive flow rate. Higher abrasive flow rates, however, cause abrasives to clash and lose their kinetic energy. It is obvious that in the jet entrance the surface is smoother and subsequently becomes rougher towards the jet exit.

4.0 References

1. Azmir MA, Ahsan AK, Rahmah A, Noor MM, Aziz AA. Optimization of abrasive water jet machining process parameters using orthogonal array with grey relational analysis. In Regional conference on engineering mathematics, mechanics, manufacturing & architecture (EM3ARC); 2007. p. 21-30.
2. Aich U, Bandyopadhyay A, Banerjee S. A state of the art-review on abrasive water jet machining process. Int Rev Mech Eng. 2013; 7:1471-1494.

3. Khan MA, Soni H, Mashinini P, Uthayakumar M. Abrasive water jet cutting process form machining metals and composites for engineering applications: A review. Eng Res Exp. 2021; 3(2):022004. https://doi.org/10.1088/2631-8695/abfe98
4. Niranjan CA, Srinivas S, Ramachandra M. Effect of process parameters on depth of penetration and topography of AZ91 magnesium alloy in abrasive water jet cutting. J Magnes Alloy. 2018; 6(4):366-374. https://doi.org/10.1016/j.jma.2018.07.001
5. Štefek A, Tyč M. Impact of preparation of titanium alloys on their abrasive water jet machining. Materials. 2021; 14(24):7768. https://doi.org/10.3390/ma14247768 PMid:34947362 PMCid:PMC8703524
6. Karmiris-Obratański P, Karkalos NE, Kudelski R, Papazoglou EL, Markopoulos AP. Experimental study on the correlation of cutting head vibrations and Kerf characteristics during abrasive waterjet cutting of titanium alloy. Procedia CIRP. 2021; 101:226-229. https://doi.org/10.1016/j.procir.2020.11.011
7. Wang J. Predictive depth of jet penetration models for abrasive waterjet cutting of alumina ceramics. Int J Mech Sci. 2007; 49(3):306-316. https://doi.org/10.1016/j.ijmecsci.2006.09.005
8. Akkurt A, Kulekci MK, Seker U, Ercan F. Effect of feed rate on surface roughness in abrasive waterjet cutting applications. J Mater Process Technol. 2004; 147(3):389-396. https://doi.org/10.1016/j.jmatprotec.2004.01.013
9. Mesalamy ASE, Youssef A. Enhancement of cutting quality of abrasive waterjet by using multipass cutting strategy. J Manuf Process. 2020; 60:530-534. https://doi.org/10.1016/j.jmapro.2020.10.036
10. Mitchell BR, Demian SAR, Korkolis YP, Kinsey BL. Experimental comparison of material removal rates in abrasive waterjet cutting and a novel droplet stream technique. Procedia Manuf. 2020; 48:586-592. https://doi.org/10.1016/j.promfg.2020.05.085
11. Liao Z, Sanchez I, Xu D, Axinte D, Augustinavicius G, Wretland A. Dual-processing by abrasive waterjet machining—A method for machining and surface modification of nickel-based superalloy. J Mat Process Technol. 2020; 285:116768. https://doi.org/10.1016/j.jmatprotec.2020.116768
12. Kowsari K, Nouraei H, James DF, Spelt JK, Papini M. Abrasive slurry jet micro-machining of holes in brittle and ductile materials. J Mat Process Technol. 2014; 214(9):1909-1920. https://doi.org/10.1016/j.jmatprotec.2014.04.008
13. Kowsari K, Sookhaklari MR, Nouraei H, Papini M, Spelt JK. Hybrid erosive jet micro-milling of sintered ceramic wafers with and without copper-filled through-holes. J Mat Process Technol. 2016; 230:198-210. https://doi.org/10.1016/j.jmatprotec.2015.11.027
14. Jain NK, Jain VK. Modeling of material removal in mechanical type advanced machining processes: A state-of-art review. Int J Mach Tools Manuf. 2001; 41(11):1573-1635. https://doi.org/10.1016/S0890-6955(01)00010-4
15. Veerappan G, Ravichandran M. Experimental investigations on abrasive water jet machining of nickel-based superalloy. J Brazilian Soc Mechan Sci Eng. 2019; 41(11)1-12. https://doi.org/10.1007/s40430-019-2031-1
16. Guha A, Barron RM, Balachandar R. An experimental and numerical study of water jet cleaning process. J Mat Process Technol. 2011; 211(4):610-618. https://doi.org/10.1016/j.jmatprotec.2010.11.017